J. Math. Biol.
DOI 10.1007/s00285-011-0487-4

Mathematical Biology

A finite-element model for healing of cutaneous wounds combining contraction, angiogenesis and closure

F. J. Vermolen · E. Javierre

Received: 14 December 2010 / Revised: 7 June 2011

Abstract A simplified finite-element model for wound healing is proposed. The model takes into account the sequential steps of dermal regeneration, wound contraction, angiogenesis and wound closure. An innovation in the present study is the combination of the aforementioned partially overlapping processes, which can be used to deliver novel insights into the process of wound healing, such as geometry related influences, as well as the influence of coupling between the various existing subprocesses on the actual healing behavior. The model confirms the clinical observation that epidermal closure proceeds by a crawling and climbing mechanism at the early stages, and by a stratification process in layers parallel to the skin surface at the later stages. The local epidermal oxygen content may play an important role here. The model can also be used to investigate the influence of local injection of hormones that stimulate partial processes occurring during wound healing. These insights can be used to improve wound healing treatments.

Keywords Wound healing · Finite-element method · Wound closure · Wound contraction · Angiogenesis

Mathematics Subject Classification (2000) 35L65 · 92C99

F. J. Vermolen (✉)
Delft Institute of Applied Mathematics,
Delft University of Technology, Delft, The Netherlands
e-mail: F.J.Vermolen@tudelft.nl

E. Javierre
Centro Universitario de la Defensa-AGM, Zaragoza, Spain

E. Javierre
Aragón Institute of Engineering Research (I3A),
Universidad de Zaragoza, Zaragoza, Spain

Published online: 10 November 2011

1 Introduction

Wound healing is a crucial process for each organism to keep its integrety and viability. The biological mechanisms behind wound healing have been investigated for a long time, yet a full understanding of this very complicated process has never been reached. For a historical review on wound healing research, which was even a scientific topic among the ancient Egyptians, we refer to Murray (2004). As many current studies are clinical, we believe that mathematical models may help to give insight into the understanding of the biological processes and the coupling between these processes that facilitate wound healing.

The human skin covers the human body, and protects the human body against the invasion of hazardous chemicals, against mechanical damage, and against heat or cold. The skin consists of several layers, all with their own function, biological composition and properties. Roughly speaking, we distinguish the following layers from the surface to the bottom: the *epidermis*, *dermis* and *subcutis*. The epidermis is known to consist of five layers. The top layer, serving as a first protection, consists of dead flat *keratinocytes* and is referred to as the *corneum*. The epidermis predominantly consists of *keratinocytes*. The second layer, the dermis, mainly consists of *fibroblasts*, *collagen* or *extracellular matrix (ECM)*, *macrophages* and *capillaries*, which are constructed from *endothelial cells*. The third layer, the subcutis, mainly consists of fibroblasts and *adipocytes*, which store nutrients and fat, and capillaries. Hence, when a deep wound, occurs so that the dermis is damaged, then, the blood vessels are cut and blood enters the wound gap. The platelets generate a fibrin network (blood coagulation), which closes the wound temporarily and due to this clot, the blood vessels are closed as well, by which excessive loss of blood (bleeding) is prevented. Subsequently, contaminants are removed from the wounded area and platelets start to secrete inflammatory chemicals which signal the occurrence of the wound, by which the cells in the surrounding tissues are activated. This activation will initiate tissue repair and regeneration of the blood vessel network, which is needed to supply the tissue with oxygen and nutrients, to facilitate important mechanisms like cell proliferation, collagen regeneration and cell mobility. The important and complicated biological process of cutaneous (dermal and epidermal) wound healing is known to proceed by a combination of various processes: wound contraction (pulling forces exerted by the (myo)fibroblasts on the ECM during the regeneration of the dermis), chemotaxis (cellular movement induced by a concentration gradient), angiogenesis, secretion of signaling agents by the platelets, synthesis of ECM proteins, and scar remodeling. A sketch of wound healing, which incorporates the aforementioned processes, is shown in Fig. 1. A description in medical terms can, among many others, be found in Stadelman et al. (1997) and Lamme (1999), and their listed references. Further, an interesting reference on general mathematical issues in biology is provided in de Vries et al. (2006).

In most of the mathematical models for (epi)dermal wound healing in literature, such as Adam (1999), Arnold (2001), Sherratt and Murray (1991), Wearing and Sherratt (2000), Friesel and Maciang (1995), Gaffney et al. (2002), Stoletov et al. (2002), Maggelakis (2003, 2004), Olsen et al. (1995), Pettet et al. (1996), and Javierre et al. (2009b), to mention a few, only one process during wound healing is modeled. However, according Stadelman et al. (1997), these sequential processes overlap

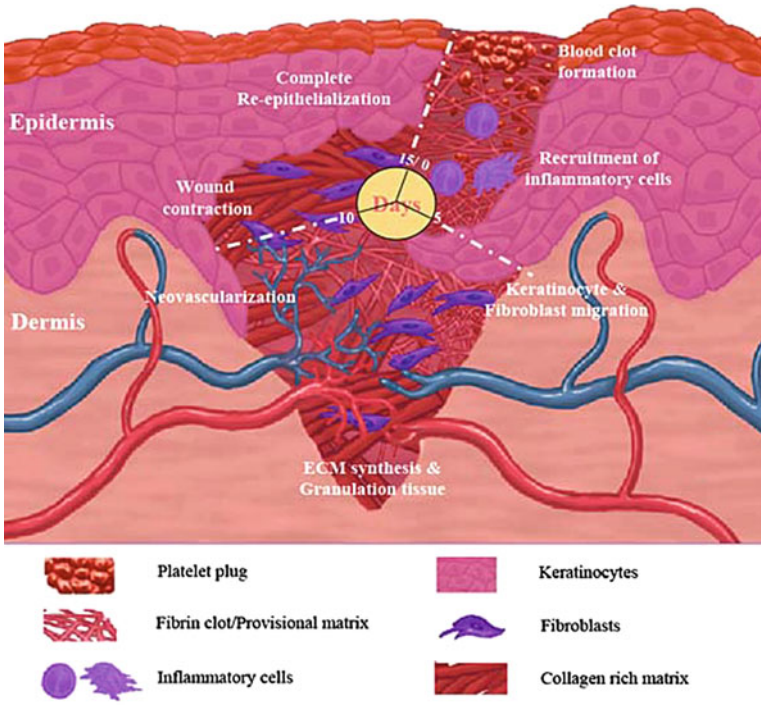

Fig. 1 A schematic of the events during wound healing. The dermis, epidermis and blood clot are illustrated. Fibroblasts move into the blood clot occupied area. The picture was taken with permission from http://www.bioscience.org/2006/v11/af/1843/figures.htm.

at least partly. In some of these references, wound healing is treated as a moving boundary problem in which the wound edge is followed explicitly. This is also done in studies on tumor growth, as in Hogea et al. (2006), where the level set method is used to track the tumor boundary. In Schugart et al. (2008), Xue et al. (2009), Vermolen and Adam (2007), Javierre et al. (2008), Vermolen (2009), Vermolen and Javierre (2009b, 2010), several attempts were made to combine these partial processes to get a more complete model for dermal wound healing. In Schugart et al. (2008) and Xue et al. (2009), the models focused on angiogenesis and dermal regeneration, but visco-elastic effects were left out. Whereas, in Vermolen and Adam (2007) and Vermolen (2009), it was focused on a combination of angiogenesis and reepithelialization (closure of the epidermis). In Vermolen and Javierre (2009b), a literature review on mathematical models for cutaneous wound healing is presented. Whereas, in Vermolen and Javierre (2010), the first attempt to combine the three processes on dermal regeneration, including visco-elastic effects from wound contraction, and angiogenesis, both taking place in the dermis. Wound closure is modeled to actually take place in a separate layer, the epidermis, in the domain of computation. The paper (Vermolen and Javierre 2010) was devoted to an tissue engineering audience, and therefore, the mathematical relations were not presented therein, and the lastmentioned paper was more descriptive about the implications of the model. In the present

paper, we will introduce the partial differential equations (PDEs) that were solved in Vermolen and Javierre (2010), describe their motivation, and solution procedure. Furthermore, we will describe the implications. The current model, as described in this manuscript, has been extended with respect to Vermolen and Javierre (2010), in terms of a coupling from angiogenesis to dermal regeneration and contraction. This revision is a result of discussions with physicians. In Vermolen and Javierre (2010), angiogenesis was only assumed to depend on dermal tissue regeneration, and not the other way around. The signaling processes due to secretion of agents by the platelets and growth factors by the fibroblasts to initiate keratinocyte proliferation to close the epidermis, are not incorporated in the present model, and in this way, these processes are assumed to proceed instantaneously. Models for the signaling processes, are, among others, presented in studies due to Wearing and Sherratt (2000), Friesel and Maciang (1995) and Stoletov et al. (2002), for keratinocyte signaling, angiogenesis, and signaling for mobilizing of fibroblasts, respectively. Here, we also mention some *continuum* models for angiogenesis, which is an essential process within wound healing. Some studies were done by Schugart et al. (2008), Maggelakis (2004) and Gaffney et al. (2002), to mention a few. The model due to Schugart et al. (2008) sets up a complete picture for dermal wound healing in the sense that the fibroblasts, extracellular matrix, inflammatory cells, capillary sprouts and tips are taken into account. However, no mechanical aspects such as wound contraction are incorporated in their model. Chronic wounds are studied by Xue et al. (2009), in which a comparison is made between ischemic and 'normal' wounds. Other work of interest in this framework, concerns the studies in enterocyte layer migration, in which a nonlinear diffusion problem is derived and solved with a one-dimensional finite-difference method. This study is due to Mi et al. (2007). Swigon et al. (2010) derive and solve a Stefan-like (diffusion with a moving boundary based on a conservation argument) problem to deal with the migration of sheets of cells. This is applied to epithelial sheet migration.

Next to the continuum models that are mostly based on PDEs, a large variety of models, based on a discrete cellular level, exist. In this framework, we mention the work due to Dallon and Ehrlich (2008) and Dallon (2010), in which several modeling approaches are presented and discussed. One such an approach is the Cellular Potts model, due to Graner and Glazier (1992), which is used to simulate biological processes, such as vascularization around tumors. Vascularization has been modeled using the cellular potts model extensively by Merks et al. (2009), among others. The cellular potts model is a lattice based model in which each pixel can represent a cell and hence falls within the class of *discrete* cellular automata models. In the cellular potts model, the driving force of the movement of the cells is a Hamiltonian, that is an energy, which determines the probability of allowing a lattice change in terms of the positions of the entities (in most biological cases individual cells). The update is done using a Monte-Carlo like algorithm.

The current manuscript should be regarded as descriptive in terms of the mathematical model and some of its implications. The results that are presented in the present study are qualitative and a quantitative description is beyond the scope of the paper since many parameters are not exactly known. Further, the current paper does not aim at being formal in a mathematical sense, as the obtained equations are hardly analyzed here. This has partly been done in earlier studies for the submodels, see Murray (2004),

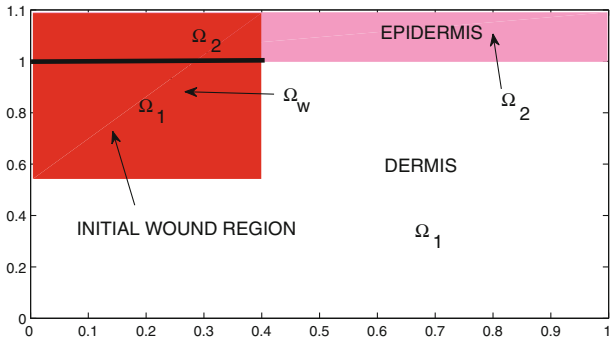

Fig. 2 The geometry of the model with the dermis and epidermis. In the dermis, the levels of fibroblasts, extra cellular matrix, oxygen, nutrients, vascular endothelial growth factor and capillaries are monitored. In the epidermis, the oxygen, nutrients, keratinocyte (epidermal cell) and epidermal growth factor levels are tracked

Sherratt and Murray (1991) and Maggelakis (2003) of which we used the simplified models. The present paper attempts to describe and simulate wound healing by coupling the processes of wound contraction (dermal regeneration), angiogenesis, and epidermal closure, and to use simple models for each subprocess. In a future manuscript, we intend to present a mathematical analysis of the contraction model based on visco-elasticity. The analysis will be carried out in the same mathematical rigor as in Vermolen and Javierre (2009a). The most important innovation of the present work is the mathematical description of the coupling of the several processes during cutaneous wound healing (wound contraction/dermal regeneration, angiogenesis and wound closure) and a revision of the model of which some implications were presented in Vermolen and Javierre (2010).

The present paper, which contains modeling wound healing by the use of the *continuum hypothesis*, is organized as follows. First, the mathematical model for wound contraction, angiogenesis and wound closure is presented. The model consists of a coupling of all these partial processes. Second, the numerical method is described. Then, some results are presented in which all simulations were done for the complete model, which consists of a coupling of all submodels for angiogenesis, wound contraction and wound closure. This is followed by a discussion. We end up with some concluding remarks.

2 The mathematical model

In this section a model, in terms of a system of PDEs, initial and boundary conditions, for cutaneous wound healing is presented. The model incorporates wound contraction, neo-vascularization and wound closure. The construction of the model relies on a combination of the ideas developed by Tranquillo and Murray (1992), Maggelakis (2004), Gaffney et al. (2002) and Sherratt and Murray (1991). The formation of the microvascular network is assumed to be triggered by a shortage of oxygen on the wound sites. In Fig. 2, a schematic of the hypothetical wound geometry and surrounding tissues is shown.

The domain of computation is given by $\Omega = \Omega_1 \cup \Omega_2 \cup (\overline{\Omega}_1 \cap \overline{\Omega}_2)$, where Ω_1 and Ω_2 respectively denote the open region occupied by the dermis and epidermis respectively. Here, $\Omega_1 := (0, L_x) \times (0, L_y)$ and $\Omega_2 := (0, L_x) \times (L_y, L_y + \delta)$, where δ denotes the thickness of the epidermis. The overbar indicates the closure of a (sub-)domain. Further the overall initial wounded region is denoted by Ω_w, which contains parts of the epidermal and dermal region. Hence $\Omega_w \cap \Omega_1$ and $\Omega_w \cap \Omega_2$, respectively, denote the initial wounded regions within the dermis and epidermis. We emphasize that in the present paper, the simplest models for each subprocess, being wound contraction, angiogenesis, and wound closure, are used.

2.1 Wound contraction

To simulate wound contraction, we use and extend the model due to Tranquillo and Murray, as described in Murray (2004). After post-traumatic coagulation of blood, the wound is closed so that a less significant number of contaminants are able to enter the wound area, and connective tissue fills the wound gap. At the consecutive stage chemically mobilized fibroblasts enter the dermal gap and start to proliferate up to an equilibrium density. The transport is modeled by a diffusive flux, which is influenced by the local strain pattern. The incoming fibroblasts regenerate an extracellular matrix on which they exert a contractile force. All equations in this subsection apply to the dermis part of the domain of computation, hence to subdomain Ω_1. The fibroblast balance becomes

$$\frac{\partial c_{fib}}{\partial t} + \operatorname{div}(\mathbf{u}_t c_{fib}) = \nabla \cdot \left(\mathbf{D}_{fib} \frac{c_o^2}{c_\theta^2} \nabla c_{fib} \right) + r c_{fib} \left(1 - \frac{c_{fib}}{c_{fib}^0} \right). \tag{1}$$

Here c_{fib}, c_0, $\mathbf{D}_{fib}$, $\mathbf{u} = \langle u, v \rangle$, r and c_{fib}^0 respectively denote the fibroblast density, oxygen concentration, motility tensor, displacement vector with horizontal and vertical components given by u and v, respectively, proliferation rate and equilibrium fibroblast density as in the unwounded state. Furthermore, c_θ denotes the dermal equilibrium oxygen content. The accumulation rate of the fibroblasts in the dermis, see the first term in the left-hand side of Eq. 1, is determined by cell motility, and cell proliferation, see the first and second terms in the right-hand side of Eq. 1, respectively. We will explain these two terms.

– Fibroblast motility (first term in the right-hand side of Eq. 1): The motility is assumed to increase quadratically with the oxygen content. This quadratic relation is assumed to make the decrease of fibroblast mobility more significant if the oxygen content is low than just by a linear relation. In the study of Vermolen and Javierre (2010), the fibroblast regeneration was assumed not to depend on oxygen, and hence the dermal regeneration was assumed to be insensitive to angiogenesis. Hence the present incorporation of the oxygen tension into fibroblast motility is an extension with respect to the earlier work (Vermolen and Javierre 2010). Of course, as the oxygen content exceeds a certain threshold, then the increase of the fibroblast mobility should go to a limit. This is not incorporated in the present model since the oxygen content does not exceed c_θ. Further, the motility of the

fibroblasts is determined by strain-biased motion, which we will specify a bit later in terms of a relationship between the motility and local strain.
– Cell proliferation (second term in the right-hand side of Eq. 1): The fibroblasts divide until they reach an equilibrium of c^0_{fib} in a logistic manner. The division rate constant r has a unit of s^{-1}.

The second term on the left-hand side in Eq. (1) follows from a passive convection of the cells due to the deformation of the structure. Note that Eq. (1) is of Fisher–Kolmogorov type, which in the absence of passive convection admits solutions with a traveling wave structure. The mechanism of fibroblast differentiation to myofibroblasts has not yet been taken into account as was done in Olsen et al. (1995) and Javierre et al. (2009a). Biologically, one could interpret our simplified approach as assuming that c_{fib} models the density of both fibroblasts and myofibroblasts. Then, the difference in the exertion of contraction and in the mobility are not taken into account here. According to Murray (2004), the motility tensor depends on the local strain in the following way

$$\mathbf{D_p} = \frac{D^0_p}{2} \cdot \begin{pmatrix} 2+\varepsilon_{xx}-\varepsilon_{yy} & 2\varepsilon_{xy} \\ 2\varepsilon_{xy} & 2+\varepsilon_{yy}-\varepsilon_{xx} \end{pmatrix}, \quad \text{where } p \text{ denotes the cell type.} \tag{2}$$

The cell types considered are fibroblasts, endothelial cells (via the capillary density) and keratinocytes (in the epidermis). For the relation between the strain ε and displacements (u and v), we use the following simple relationship:

$$\varepsilon(u, v) := \begin{pmatrix} \frac{\partial u}{\partial x} & \frac{1}{2}\left(\frac{\partial u}{\partial y} + \frac{\partial v}{\partial x}\right) \\ \frac{1}{2}\left(\frac{\partial u}{\partial y} + \frac{\partial v}{\partial x}\right) & \frac{\partial v}{\partial y} \end{pmatrix}.$$

The production of extra cellular matrix (ECM) by the fibroblasts is modeled by

$$\frac{\partial c_{ecm}}{\partial t} + \operatorname{div}(\mathbf{u}_t c_{ecm}) = b c_{fib}\left(1 - \frac{c_{ecm}}{c^0_{ecm}}\right). \tag{3}$$

Here b, c_{ecm} and c^0_{ecm} respectively represent the ECM production rate in s^{-1}, ECM density and equilibrium ECM density. Once again the second term in the left-hand side accounts for passive convection. The right-hand side is based on the assumption that the production rate is proportional to the density of fibroblasts. Furthermore, the production rate of collagen decreases as the extra cellular matrix density increases towards its equilibrium value. It can be shown that $c_{ecm} = c^0_{ecm}$ and $c_{fib} = c^0_{fib}$ are stable steady-state solutions under $\operatorname{div} \mathbf{u}_t = 0$. Therefore, the undamaged state is stable.

Before we deal with the mechanical balance equations, we first introduce the indicator function in order to be able to make a distinction between the epidermis and dermis if it concerns the reaction forces resulting from pulling behavior of fibroblasts in the dermis. Let $V \subset \Omega$ be non-empty, then we define the indicator function,

$\chi_V(x, y) : \Omega \to \{0, 1\}$, where $V \subset \Omega$, by

$$\chi_V(x, y) = \begin{cases} 1, & \text{if } (x, y) \in V, \\ 0, & \text{if } (x, y) \in \Omega \backslash V. \end{cases} \tag{4}$$

For the force equilibrium, we have the following equation at a certain time

$$-\operatorname{div} \sigma = c_{ecm}\mathbf{F} \cdot \chi_{\Omega_1}(x, y), \qquad (x, y) \in \Omega, \tag{5}$$

where σ denotes the stress tensor and $\mathbf{F}$ represents mass-spring body force as a reaction to the pulling exerted on the extracellular matrix. This mass-spring force acting as a body force is given by

$$\mathbf{F} = -s\mathbf{u}. \tag{6}$$

Here, s denotes the tethering elasticity coefficient, which quantifies the resistance of the attached tissue matrix. We note that the cell traction and spring force are nonzero in the dermis domain only, that is in Ω_1. Further, c_{ecm} denotes the ECM density. The use of the indicator function mimics the presence of the reaction spring forces in the dermis only. The stress contains the following components: visco-elasticity [the first three terms, the first two representing viscous forces and the third term resulting from linear elasticity (Hooke's Law)] and cell traction, which is proportional to the ECM content and the fibroblast density. This gives the following mechanical force balance:

$$\sigma = \mu_1 \varepsilon_t + \mu_2(\nabla \cdot \mathbf{u}_t)\mathbf{I} + \frac{E}{1+\nu}\left[\varepsilon + \frac{\nu}{1-2\nu}(\nabla \cdot \mathbf{u})\mathbf{I}\right] + \frac{\tau c_{fib} c_{ecm}}{1 + \lambda c_{ecm}^2}\mathbf{I}. \tag{7}$$

Here μ_1, μ_2, E and ν respectively denote viscosity (the dynamic and kinematic viscosity), Young's modulus and Poisson's ratio. Further, $\mathbf{I}$ denotes the identity tensor. In the present study, we assume that the stiffness of the tissue does not depend on strain. In principle, a hyper-elastic model would be more appropriate. However, such a behavior is not included in the present study since we want the current model to be as simple as possible as it is already sufficiently complex as it contains a combination of the simplest models for each subprocess. The stress that is exerted by one fibroblast on the extracellular matrix is denoted by τ. The traction saturation constant is denoted by λ, and it warrants the existence of a ECM density for which the ECM production is maximal, so that a larger value moves the stress-maximizing fibroblast density towards zero and additionally decreases the actual maximum fibroblast density.

Initially all densities are zero in the wounded region and initially the displacement $\mathbf{u} = \mathbf{0}$ is also zero in Ω. Further, far away from the wound, the displacement is assumed to be zero as a boundary condition and at $x = 0$, which is the line of symmetry, the displacement in the x-direction vanishes, that is $u = 0$. At the bottom of the domain of computation, we have $v = 0$. At the top of Ω (that is at the top of the epidermis), we assume the traction to be zero, which gives a free boundary. Further, the fibroblasts are subject to a no-flux boundary condition.

As initial conditions, we use

$$c_{fib}(x, y, 0) = \begin{cases} 0, & \text{for } (x, y) \in \Omega_w \cap \Omega_1, \\ c^0_{fib}, & \text{for } (x, y) \in \Omega_1 \backslash \Omega_w, \end{cases} \tag{8}$$

for the fibroblasts. For the ECM, we use initially

$$c_{ecm}(x, y, 0) = \begin{cases} 0, & \text{for } (x, y) \in \Omega_w \cap \Omega_1, \\ c^0_{ecm}, & \text{for } (x, y) \in \Omega_1 \backslash \Omega_w. \end{cases} \tag{9}$$

2.2 Angiogenesis

The model that we use for this partial process was presented in Maggelakis (2004), as it is one of the simplest models that incorporate the actual initiation of angiogenesis as a result of a lack on oxygen. Angiogenesis is a crucial process for tissue regeneration and for tumor growth (Rossiter et al. 2004). It is assumed that the capillaries and its tips act as the only sources for oxygen supply. Due to the injury, the microvascular network is damaged in the wound area and as a result the oxygen concentration decreases there. This lack of oxygen initiates macrophage activation, which among other tasks, such as being scavengers or admirals to remove harmful bacteria and chemicals, start producing the macrophage derived growth factors (MDGF), such as vascular endothelial growth factors (VEGF). These growth factors make the endothelial cells proliferate, which induces the regeneration of capillaries and thereby the vascular network is restored. In the experimental work of Rossiter et al. (2004), it is revealed that loss of VEGF's causes an enormous delay in healing time of deep wounds due to the presence of blood vessel-free zones. Their findings are sustained by animal experiments on mice.

Due to the regeneration of capillaries, the oxygen concentration increases, causing the production of new capillaries to be inhibited. The flow chart of this negative feedback mechanism is sketched in Fig. 3.

Let c_o and c_c respectively denote the oxygen concentration and the capillary density and let them be functions of time t and space within the entire domain of computation Ω and the dermis region Ω_1, respectively; then a mass balance results into the following PDE:

$$\frac{\partial c_o}{\partial t} + \text{div}(\mathbf{u}_t c_o) = \nabla \cdot (D_o \nabla c_o) - \lambda_o c_o + \lambda_{o,c} c_c, \quad \text{for } (x, y) \in \Omega. \tag{10}$$

Here D_o, λ_o, and $\lambda_{o,c}$, respectively denote the diffusivity of oxygen, the natural decay rate coefficient of oxygen, and the increase rate of oxygen per number of capillaries in a unit volume. Assuming a consolidation of the scaffold after some of bleeding, it is reasonable to suppose that the main part of oxygen has been consumed in the wound area. Therefore, we set the initial oxygen concentration zero there. Further, in the undamaged tissue there is an equilibrium profile of oxygen. Therefore, the initial concentration of oxygen is determined by the combination of the steady-state of the

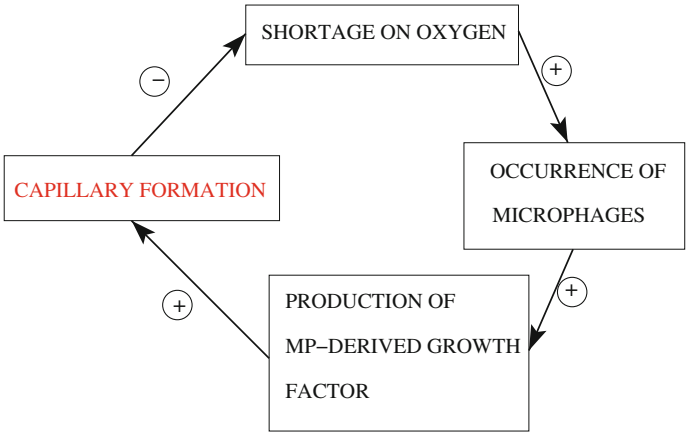

Fig. 3 A schematic of the negative feedback mechanism for the model for angiogenesis due to Maggelakis

oxygen concentration profile according to the undamaged state and the zero level in the damaged state. Hence the initial oxygen concentration profile is determined by

$$c_o(x, y, 0) = \begin{cases} \tilde{c}_o(x, y), & \text{for } (x, y) \in \Omega \backslash \Omega_w, \\ 0, & \text{for } (x, y) \in \Omega_w. \end{cases} \tag{11}$$

The equilibrium profile of oxygen in the undamaged tissue, indicated by the function $\tilde{c}_o$ will be specified after the treatment of the capillary density. For completeness, we also note that the capillaries do not enter the epidermal region.

It is assumed that there is no transport of oxygen over the symmetry boundary and on boundaries that are far away from the wound. As well as, it is assumed that no oxygen enters from the dermis into the subcutis via diffusion. This assumption is probably an oversimplification of reality, and it can be relaxed easily. This boundary condition will not provide significant changes in the qualitative picture of cutaneous wound healing that we want to present in the current paper. Oxygen is allowed to enter the epidermis via diffusion through the basal membrane. The diffusivity in the basal membrane is not adjusted. This results into a homogeneous Neumann boundary condition for oxygen at all boundaries of the domain of computation. The above equation is based on the assumption that the oxygen supply and oxygen consumption depend linearly on the capillary density and oxygen concentration respectively. Since oxygen reaches the tissue predominantly via the capillaries, and hardly from the contact between the epidermis and the outer surroundings, it is reasonable to neglect the transport of oxygen over the outer skin boundary which is in contact with the surroundings. Since oxygen transport is determined by diffusion only, we use a homogeneous Neumann boundary condition on the top of the epidermis.

As mentioned earlier, if the oxygen level is low, then macrophages start releasing VEGF to initiate regeneration of blood vessels and collagen deposition. The skin tissue is then provided with necessary nutrients and oxygen for cell division needed for wound closure. An assumption in the model is that VEGF is produced if the oxygen

level is below a threshold value, say c_θ. The VEGF-production rate, Q, is assumed to depend linearly on the lack of oxygen, that is

$$Q = Q(c_o) = \begin{cases} 1 - \dfrac{c_o}{c_\theta}, & \text{if } c_o < c_\theta, \\ 0, & \text{if } c_o \geq c_\theta. \end{cases} \tag{12}$$

The number of macrophages is assumed to be homogeneously distributed in undamaged tissue, so the actual natural density of macrophages is hidden in the production rate Q. The mass balance of VEGF's, its concentration being denoted by c_v, results into the following PDE's in the wounded dermal region $\Omega_w \cap \Omega_1$ and out of the wound region $\Omega_1 \backslash \Omega_w$:

$$\begin{aligned} \frac{\partial c_v}{\partial t} + \operatorname{div}(\mathbf{u}_t c_v) = \nabla \cdot (D_v \nabla c_v) + \lambda_{v,o} \frac{\left(\frac{c_{fib}}{c^0_{fib}}\right)^2}{\tau_v + \left(\frac{c_{fib}}{c^0_{fib}}\right)^2} Q(c_o) \\ -\lambda_v c_v, \quad \text{for } (x, y) \in \Omega_w \cap \Omega_1, \end{aligned} \tag{13}$$

Here, D_v, $\lambda_{v,o}$, λ_v, and c^0_{fib}, respectively, denote the diffusion coefficient of VEGF in the tissue, the VEGF production rate coefficient by the macrophages, natural decay rate of VEGF, and the fibroblast density in undamaged tissue. The parameter τ_v will be explained a little later in this section. The three terms in the right-hand side mimic VEGF diffusion, VEGF production by macrophages, and natural decay, respectively. The reasoning behind this model equation is similar to tumors secreting growth factors to enhance vascularization around the tumor, see Balding and McElwain (1985) and Mantzaris et al. (2004) as examples. It is assumed that angiogenesis and the associated production of MDGF takes place in the (partially) restored dermis only, as both macrophages and fibroblasts enter the wound area. Although the motilities of fibroblasts and macrophages differ, we assume that their motilities are comparable and that the number of *actively* VEGF producing macrophages is coupled to the quality of the dermis. The quality of the dermis is assumed to be measured by the fibroblast density. One could argue to incorporate also the level of the collagen content in the measure for the dermal quality. However, as the contents of fibroblasts and collagen are closely related, we decided to use the fibroblast density only to make the model as simple as possible such that it describes biological phenomena in a sound manner. In a restored dermis, the normalized fibroblast $\frac{c_{fib}}{c^0_{fib}}$ density equals one, whereas in a totally disrupted dermis the fibroblast density vanishes. Therefore, the function of c_{fib} is introduced in front of the VEGF regeneration term. It would probably be more appropriate to incorporate the macrophage density there too. This would require the extra tracking of the macrophages and hence make the model more complicated. Therefore, we omit this extension, and use the dermal quality as the input parameter. This function implies that the VEGF regeneration vanishes as c_{fib} is zero and increases monotonically as the fibroblast density increases. The parameter τ_v warrants that the increase of the VEGF production resembles a quadratic behavior for small values of

c_{fib} and an asymptotically flattening behavior as c_{fib} becomes very large. The larger τ_v, the less sharp the increase of the VEGF production becomes for large values of fibroblast density. The initial VEGF concentration is assumed to be zero in the entire domain of computation Ω and a homogeneous Neumann boundary condition is used, also at the basal membrane between the dermis and epidermis. The capillary density, c_c, is assumed to grow as a result of the VEGF's in a logistic manner, that is

$$\frac{\partial c_c}{\partial t} + \mathrm{div}\,(\mathbf{u}_t c_c) = \nabla \cdot (\mathbf{D}_c \nabla c_c) + \lambda_c c_v c_c \frac{\left(\frac{c_{fib}}{c^0_{fib}}\right)^2}{\tau_c + \left(\frac{c_{fib}}{c^0_{fib}}\right)^2} \times \left(1 - \frac{c_c}{c_c^{eq}\psi(\frac{c_{fib}(x,y,t)}{c^0_{fib}})}\right), \quad \text{for } (x, y) \in \Omega_1, \tag{14}$$

where c_c^{eq} denotes the equilibrium capillary density. The first term of the right-hand side models stress-biased mobility of the endothelial cells which are the building blocks for the capillaries. The last term in the right-hand side models logistic growth of the capillary density. This proliferation linearly increases with the VEGF concentration. Further, this proliferation increases with an increasing dermal quality. In the above equation, λ_c denotes the capillary proliferation rate. To incorporate the dermal quality, a similar function of the fibroblast density to the one in (13) is proposed in Eq. (14). As before, the parameter τ_c warrants that the increase of the capillary proliferation resembles a quadratic behavior for small values of c_{fib} and an asymptotically flattening behavior as c_{fib} becomes very large. It is well-known that the vascular density is slightly elevated in the vicinity of the dermal wound edge, see for instance the study by Szpaderska and DiPietro (2003), where is it claimed that the capillary density in wounded areas may reach more than twice the usual capillary density in the undamaged state. In their study they consider both oral and skin wounds. Since it has been observed that indeed the endothelial cell density, or the capillary density, is elevated with respect to equilibrium in the undamaged state, a simple logistic proliferation rate for the capillary density is not appropriate. The complicated biological mechanisms behind this observation are 'simply' dealt with by shifting the equilibrium as a result pf the dermal quality, which we determine by the fibroblast density. The elevated capillary density is modeled by adapting the equilibrium capillary density by the function ψ in the above equation. The equilibrium capillary density increases with an increasing value of ψ. To mimic an increased equilibrium capillary density at the dermal wound edge, we use

$$\psi = \psi(c) = \begin{cases} 2 - c, & \text{if } c \leq 1, \\ 1, & \text{if } c > 1. \end{cases} \tag{15}$$

We realize that this is a crude approximation. The formalism for angiogenesis due to Gaffney et al. (2002) gives the increase of the capillary (tip) density and of the capillary

tips near the wound edge in a more natural way. The lastmentioned model, however, does not take into account the shortage on oxygen as the initiator for angiogenesis. Further, the capillary density is assumed to satisfy the following initial condition

$$c_c(x, y, 0) = \begin{cases} 0, & \text{for } (x, y) \in \Omega_w \cap \Omega_1, \\ c_c^{eq}, & \text{for } (x, y) \in \Omega_1 \backslash \Omega_w. \end{cases} \tag{16}$$

A homogeneous Neumann boundary condition is used for c_c. The capillaries are assumed to grow and to 'migrate' via a random walk process. Capillary 'movement' was not incorporated into Maggelakis' model but this migration was extended with a bias in Gaffney's model by the incorporation of cross diffusion coefficients. The bias is neglected in this paper but it will be investigated in future work. Further, Gaffney et al. (2002) distinguish between the actual capillaries and the actual capillary tips. Maggelakis sets in a nonzero artificial starting value for the capillary density to have the capillary density to increase up to the equilibrium value. The original approach due to Maggelakis was simpler since her study aimed at finding explicit analytic solutions. The assumption that capillary tips migrate by random walk is also a key-assumption in the work due to Plank and Sleeman (2003, 2004).

For the initial oxygen content, we use the assumption that its value equals zero in the initial wound region. At the other locations in the computational domain, we assume it to be given by the steady-state solution of the undamaged state in the entire domain of computation, this is the function $\tilde{c}_o$ determined from

$$-D_o \Delta \tilde{c}_o + \lambda_o \tilde{c}_o = \begin{cases} \lambda_{o,c} c_c^{eq}, & \text{for } (x, y) \in \Omega_1, \\ 0, & \text{for } (x, y) \in \Omega_2. \end{cases} \tag{17}$$

It can be demonstrated from analytic considerations that $\lim_{t \to \infty} c_o(x, y, t) = \tilde{c}_o(x, y)$ in Ω.

2.3 Wound closure

In this study, we extend the model due to Sherratt and Murray (1991), which contains all the important features qualitatively. The mechanism for wound closure is mitosis: cell division and growth. We are aware of the fact that this mechanism is triggered by a complicated system of growth factors. In the present study, we follow Sherratt and many others, in which it is assumed that one epidermal growth factor regulates wound closure, which is sufficient to get the right qualitative picture of wound closure. The influence of keratinocyte growth factor signaling is neglected in the current study. The epidermal growth factors determine the regeneration of epidermal cells. If the number of epidermal cells is low, then, the epidermal cells produce an excessive amount of growth factors. Whereas, as the healed state is reached, then, the growth factor production decreases such that the healed cell concentration is stable. Following Sherratt and Murray (1991), we assume that the growth factors are exclusively generated by the epidermal cells. The epidermis-derived growth factors diffuse through the epidermis, and hence the portion of them that cross the basal membrane to enter the underlying

dermis is assumed to be negligible. Further, the epidermal growth factors are subject to natural decay. Let c_{epi} and c_{egf} respectively denote the epidermal cell density and epidermal growth factor concentration, then the adapted expression of Sherratt and Murray where the accumulation of the epidermal cells is determined by proliferation (diffusive transport), mitosis and cell death, in Ω_1, is given by

$$\frac{\partial c_{epi}}{\partial t} + \mathrm{div}(\mathbf{u}_t c_{epi}) = \nabla \cdot (\mathbf{D}_{epi} \frac{c_o^2}{\tau_o + c_o^2} \nabla c_{epi}) + s(c_{egf}) \phi(c_o) c_{epi} \left(2 - \frac{c_{epi}}{c_{epi}^{eq}} \right) - \lambda_{epi} c_{epi},$$
$$\text{subject to } c_{epi}(x, y, 0) = \begin{cases} 0, & \text{for } (x, y) \in \Omega_w \cap \Omega_2, \\ c_{epi}^{eq}, & \text{for } (x, y) \in \Omega_2 \backslash \Omega_w. \end{cases} \tag{18}$$

In the above PDE, the right-hand side consists of keratinocyte stress-biased motility, proliferation and natural decay. Here $\mathbf{D}_{epi}$, λ_{epi} and τ_o, respectively, denote the stress-biased diffusion coefficient, a natural decay term, the parameter τ_c warrants that the increase of the capillary proliferation resembles a quadratic behavior for small values of c_{fib} and an asymptotically flattening behavior as c_{fib} becomes very large. The function $s = s(c_{egf})$ is nonlinear and describes the mitotic rate, see Murray (2004) and Sherratt and Murray (1991). This function will be specified later in this section. Furthermore, as the epidermal cells need oxygen and nutrients to become motile, the motility increases with increasing oxygen (c_0) and nutrients level (c_n). These dependencies are included in the above equation. Of course the behavior and need of nutrients is similar to the contribution of oxygen. Therefore, this issue is not dealt with explicitly in this paper. Note that these dependencies are just assumptions. However, we think that the picture is right from a qualitative point of view. The proliferation rate of the epidermal cells depends on the oxygen level. This is incorporated by the use of the function $\phi(c_0)$, which gives a linear dependence up to a certain maximum. This relation will be specified a bit later in this section.

For the growth factor accumulation a similar relationship due to diffusive transport, production and decay is obtained with a similar adaptation for the dependence of the capillary density:

$$\frac{\partial c_{egf}}{\partial t} + \mathrm{div}(\mathbf{u}_t c_{egf}) = \nabla \cdot (D_{egf} \nabla c_{egf}) + \phi(c_o) f(c_{epi}) - \lambda_{egf} c_{egf}, \ (x, y) \in \Omega_2,$$
$$\text{subject to } c_{egf}(x, y, 0) = \begin{cases} 0, & \text{for } (x, y) \in \Omega_w \cap \Omega_2, \\ c_{egf}^{eq}, & \text{for } (x, y) \in \Omega_2 \backslash \Omega_w. \end{cases} \tag{19}$$

Here D_{egf} and λ_{egf}, respectively, denote the diffusion coefficient of the epidermal growth factor, and a natural decay rate. In the above equation $f(c_{epi})$ denotes a nonlinear relation for the growth factor regeneration. Sherratt and Murray distinguish two different types of growth factors are considered: 1. activators; and 2. inhibitors, both

with their characteristic functions for s and f, given by

$$s(c_{egf}) = \frac{2c_m(h-\beta)c_{egf}}{c_m^2 + c_{egf}^2} + \beta, \quad \beta = \frac{1+c_m^2 - 2hc_m}{(1-c_m)^2}, \quad f(c_{epi}) = \frac{c_{epi}(1+\alpha^2)}{c_{epi}^2 + \alpha^2}, \tag{20}$$

for the activator case and by

$$s(c_{egf}) = \frac{(h-1)c_{egf} + h}{2(h-1)c_{egf} + 1}, \quad f(c_{epi}) = c_{epi}, \tag{21}$$

for the inhibitor. Here h, β and c_m are considered as known constants, and we refer to Murray (2004) for more details. The initial wounded state is unstable, so that the functions c_{epi} and c_{egf} converge to the undamaged values c_{epi}^{eq} and c_{egf}^{eq} as $t \to \infty$. So the unwounded state is stable, and the wounded state is unstable with respect to (small) perturbations. Parts of the stability analysis has already been carried out in literature, such as for the original model for epidermal healing in Sherratt and Murray (1991). Further, in Sherratt and Murray (1991), a traveling wave analysis was carried out on the equations in its original form. We also plan to consider this stability in a more mathematical setting in future work.

Furthermore, the formation of epidermal cells and their ability to produce the epidermal cell mitosis regulating growth factor are determined by the amount of oxygen and nutrients supplied. In the present study, we assume the mitotic rate to increase as the oxygen level increases. Since, the cell division and growth rate are finite, there is a maximum division rate at which the division rate is no longer sensitive with respect to an increase of oxygen supplied. Hence, this advocates for the existence of a maximum mitotic rate. To model this, we introduce for $(x, y) \in \Omega_2$:

$$\phi(c_o(x, y, t)) := \min\left(1, \frac{c_o(x, y, t)}{\tilde{c}_o(x, y)}\right), \tag{22}$$

where $\tilde{c}_o(x, y)$ is the steady-state solution of the oxygen content in the undamaged tissue at position $(x, y) \in \Omega_2$.

3 The numerical method

The PDEs are solved using the finite-element method with triangular elements and piecewise linear basis functions. For the time integration of the nonlinear PDEs, we use an IMEX (IMplicit EXplicit) method such that a toilsome stability criterion is circumvented. The method used in the present study is similar to the method in Vermolen (2009). In this section, we deal with the numerical method for the biological diffusion-reaction equations and for the mechanical visco-elastic equations.

As numerical settings, we use 50×50 gridnodes in the dermis and in the dermis. For the time-step, we use 0.01 days. Further, an enlargement of the grid resolution and

a time step decrease did not alter the results significantly. Differences were invisible in the 'eye-ball norm'.

3.1 The biological equations

For the coupled system of equations, we use an IMEX method, hence it suffices to discuss the most complicated diffusion-reaction that we encounter in the present study. We consider equations of the form

$$\frac{\partial c}{\partial t} + \mathrm{div}(\mathbf{u}_t c) = \nabla \cdot (\mathbf{D}\nabla c) + F(c((x,y),t), w((x,y),t)), \tag{23}$$

where

$$\mathbf{D} = \frac{D^0(w(x,y,t))}{2} \cdot \begin{pmatrix} 2+\varepsilon_{xx}-\varepsilon_{yy} & 2\varepsilon_{xy} \\ 2\varepsilon_{xy} & 2+\varepsilon_{yy}-\varepsilon_{xx} \end{pmatrix},$$

represents the diffusion tensor and the PDE is supplied with an initial condition and homogeneous Neumann conditions. The equation is solved using a standard Galerkin finite-element method. Further, w is assumed to be a solution determined from an other differential equation. First, using integration by parts for the divergence term, gives

$$\int_\Omega \frac{\partial c}{\partial t}\phi d\Omega + \int_{\partial\Omega} \mathbf{u}_t \cdot \mathbf{n} c\phi d\Gamma - \int_\Omega \mathbf{u}_t c \cdot \nabla\phi d\Omega + \int_\Omega \mathbf{D}\nabla c \cdot \nabla\phi d\Omega = \int_\Omega F(c,w)\phi d\Omega. \tag{24}$$

The solution c is written as a linear combination of piecewise linear basis functions $\phi_i(x,y)$, such that $c(x,y,t) = \sum_{j=1}^n c_j(t)\phi_j(x,y)$. The integrals are evaluated over each (line) element and then the element matrices are assembled into the large matrices used for the solution of the system of differential equations. The element matrices are computed using Newton–Cotes integration, which is sufficiently accurate since in the nonlinear parts the solution is only determined up to an accuracy of $O(h^2)$, if h denotes a characteristic length (say the diameter) of the elements.

The most complicated term in the above weak form, is the diffusive flux. We will work out this term in somewhat more detail. For the element matrices, we deal with $I = \int_{\Omega_e} \mathbf{D}\nabla\phi_i \cdot \nabla\phi_j d\Omega$, where Ω_e represents an element. Taking into account the strain components, we arrive at

$$I = \int_{\Omega_e} \left(D_{xx}\frac{\partial\phi_j}{\partial x} + D_{xy}\frac{\partial\phi_j}{\partial y} \right)\frac{\partial\phi_i}{\partial x} + \left(D_{xy}\frac{\partial\phi_j}{\partial x} + D_{yy}\frac{\partial\phi_j}{\partial y} \right)\frac{\partial\phi_i}{\partial y} d\Omega.$$

The above integral is numerically approximated using a Newton–Cotes quadrature rule. Of course, a Gaussian quadrature rule is more accurate in principle, however in this application in which the solution is already accurate up to a second order in space, the Gaussian rule does not increase the order of accuracy, and hence it does not give a significant improvement. Further, the high (fourth) order of the Gaussian rule will not be useful under sudden change of the coefficients. The integration of the diffusivity is performed at the previous timestep.

3.2 The visco-elastic equation

Next, we consider the visco-elastic equations and deal with a weak solution of

$$-\nabla \cdot \sigma = \mathbf{f},$$

where

$$\sigma(\mathbf{u}) = \mu_1 \frac{\partial \epsilon(\mathbf{u})}{\partial t} + \mu_2 \left(\nabla \cdot \frac{\partial \mathbf{u}}{\partial t} \right) \mathbf{I} + \frac{E}{1+\nu} \left(\epsilon(\mathbf{u}) + \frac{\nu}{1-2\nu} (\nabla \cdot \mathbf{u}) \mathbf{I} \right).$$

The above PDE represents a force balance. The first two terms in the above equation for $\sigma(\mathbf{u})$ account for viscous effects of the soft tissue. The second term set of two terms deal with elastic effects of the tissue. Further, f is an internal body force, which could be the cell traction or a spring force. We use homogeneous Dirichlet conditions for the displacements and homogeneous natural boundary conditions for the force. Also, an appropriate initial condition has to be specified for $\mu_1 \epsilon(\mathbf{u}) + \mu_2 (\nabla \cdot \mathbf{u}) \mathbf{I}$. We denote the domain of computation by Ω and its boundary by Γ. The boundary is decomposed $\Gamma = \Gamma_1 \cup \Gamma_2$, where $\Gamma_1 := \{(x, y) \in \Omega : x = 0\} \cup \{(x, y) \in \Omega : x = L_x\}$ and $\Gamma_2 := \{(x, y) \in \Omega : y = 0\} \cup \{(x, y) \in \Omega : x = L_x\}$. To this extent, we introduce the following function spaces reflecting smoothness properties and boundary conditions:

$$\begin{aligned}
U_0 &:= \{u \in H^1(\Omega) : \ u = 0 \text{ on } \Gamma_1\}, \\
V_0 &:= \{v \in H^1(\Omega) : \ v = 0 \text{ on } \Gamma_2\}, \\
U &:= C^1((0, T], U_0) \cup C^0([0, T], U_0), \\
V &:= C^1((0, T], V_0) \cup C^0([0, T], V_0).
\end{aligned}$$

Hence, the following variational formulation is derived

$$\mathbf{u} \in U \times V : \int_{\Omega} \sigma(\mathbf{u}) : \epsilon(\phi) d\Omega = \int_{\Omega} \mathbf{f} \cdot \phi d\Omega, \quad \forall \phi \in U_0 \times V_0. \tag{25}$$

In this expression, the matrix inner product is defined by

$$A : B := \sum_{i=1}^{m} \sum_{j=1}^{m} A_{ij} B_{ij},$$

where A, B are $m \times m$-matrices. Further, the scalar inner product is employed

$$\mathbf{u} \cdot \phi := u\phi_1 + v\phi_2, \quad \text{where } \phi = [\phi_1, \phi_2]^T.$$

The PDEs are solved using a Galerkin finite-element method with linear triangles. For the time integration of the nonlinear PDEs, a backward (implicit) Euler method is applied such that a stability criterion is circumvented. We write the displacement and strain as a linear combination of the basis functions

$$\sum_j \epsilon^k_{xx,j} \int_\Omega \phi_i \phi_j d\Omega = \sum_j c^k_j \int_\Omega \phi_i \frac{\partial \phi_j}{\partial x} d\Omega, \quad \forall i \in \{1, \ldots, N\},$$

where k denotes the time index. At each time-step this system of equations is solved. Here, Newton–Cotes integration lumps the matrix to a diagonal matrix, which makes the solution of the linear system of equations very cheap. The other terms for the strain tensor are treated analogously.

4 Results for the coupled model

In the simulations, we use the following default data, which are predominantly obtained from the references in which the original submodels were described. The data can be found in Table 1. With respect to the data for the angiogenesis model, we could not find any sensible parameter values for oxygen diffusion and VEGF. For oxygen diffusion, we used a value according to the range of measured values of MacDougall and McCabe (1967). We assume that the diffusivity of VEGF is comparable to the oxygen diffusivity and therefore, we set them equal in our present study. For the reaction rate coefficients, no data was available either and therefore, we made educated guesses for them. Further, we consider a wound of the following dimensions: 0.5 cm $\times$ 0.5 cm in the dermis and of 0.1 cm $\times$ 0.5 cm in the epidermis. Hence the initial wound region is given by $(x, y) \in [0, 0.5] \times [0.5, 1, 1]$ with $\delta = 0.1$ for the thickness of the epidermis. The mechanical parameters were obtained from Murray (2004).

We finally remark that all simulations were done for the complete model.

4.1 Wound contraction simulations

To illustrate the contraction phase, that is the reparation of the dermis, we consider a wound gap on the upper left part of the dermis. Fibroblasts enter the gap region and start proliferating. Consecutively, they start producing ECM, and pulling on the ECM, which gives a contractile behavior. In Figs. 4 and 5 the fibroblast density and

Table 1 Default values in the simulations for the various parameters

Parameter	Value	Unit
L_x	1	cm
L_y	1	cm
δ	0.1	cm
c^0_{fib}	1	10^5 cells/cm^2
c^0_{cap}	0.1	10^5 cells/cm^2
c^0_{col}	1	μg/cm^3
D^0_{fib}	5.79×10^{-9}	cm^2/s
D^0_c	5.79×10^{-9}	cm^2/s
D^0_{epi}	1×10^{-8}	cm^2/s
D_o	1.16×10^{-7}	cm^2/s
D_v	1.16×10^{-8}	cm^2/s
D_{egf}	0.45×10^{-4}	cm^2/s
λ_o	2.31×10^{-7}	1/s
$\lambda_{o,c}$	2.31×10^{-5}	1/s
$\lambda_{v,o}$	2.31×10^{-6}	1/s
λ_v	2.31×10^{-9}	1/s
λ_c	1.16×10^{-4}	m^2/(s cells)
λ_{epi}	2.31×10^{-5}	1/s
λ_{egf}	3.47×10^{-4}	1/s
r	1.16×10^{-5}	1/s
b	1.16×10^{-5}	1/s
s	1×10^8	dyne s/cm^3
E	10	dyne/cm^2
ν	0.2	–
τ_o	1	–
τ_c	1	–
τ_v	1	–
τ	0.5	dyne/cell

ECM concentration are shown at several times in the inflammatory phase, in which the dermis underneath the epidermis is repaired. Furthermore, the collagen concentration is restored quickly once fibroblasts have invaded the scaffold.

The displacements were computed from the visco-elastic equations using the data in Table 1. Using these data, the displacements were very small, being in the order of 10^{-5} cm at most. Hence the displacements were not visible and we will show the displacements in the mesh points for hypothetic values of cell traction and tethering constant in the discussion section. Furthermore, from a parameter sensitivity analysis we observe:

– Near the value as specified in Murray (2004), the diffusivity parameter in front of the matrix with the strain dependence hardly influences contraction;

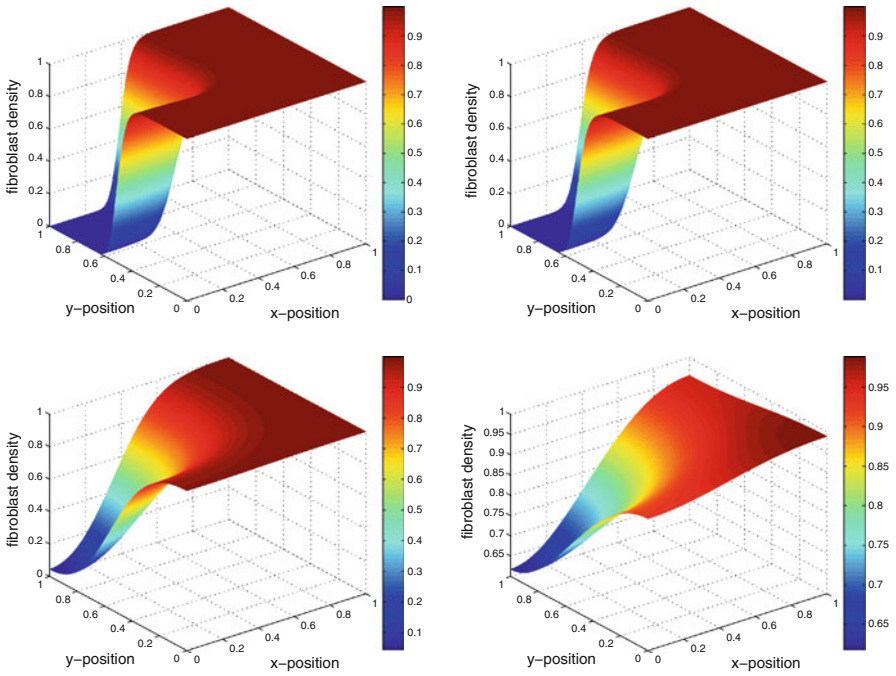

Fig. 4 The fibroblast profile in a dermal wound gap during the inflammatory phase at 5, 10, 40 and 100 days. The figures show the temporal evolution. Here, the position of the basal membrane which connects the dermis to the epidermis coincides with the line $y = 1$. The initial wound occurred at the left

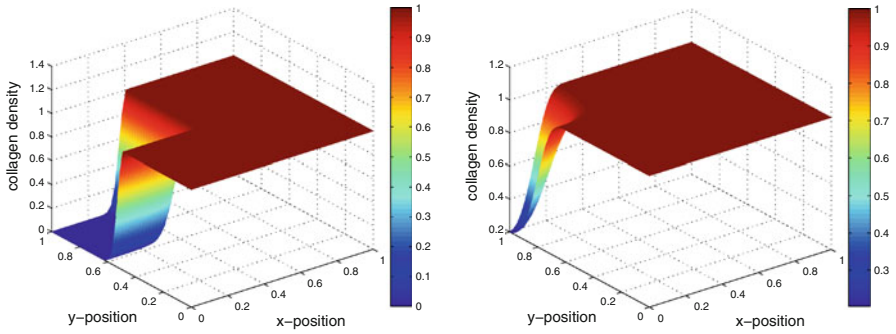

Fig. 5 The ECM profile in a dermal wound gap at 5 and 40 days. The figures show the temporal evolution. Here, the position of the basal membrane which connects the dermis to the epidermis coincides with the line $y = 1$. The initial wound occurred at the left

- Fibroblast regeneration rate coefficient (r) has some influence at later stages (low value increases contraction and decreases retraction speed);
- Collagen regeneration rate coefficient (b) has a large influence at initial and intermediate stages (initial distraction increases with decreasing b);
- Traction stress saturation (λ) has a large influence (even qualitatively initially, $\lambda = 0$ gives no initial distraction).

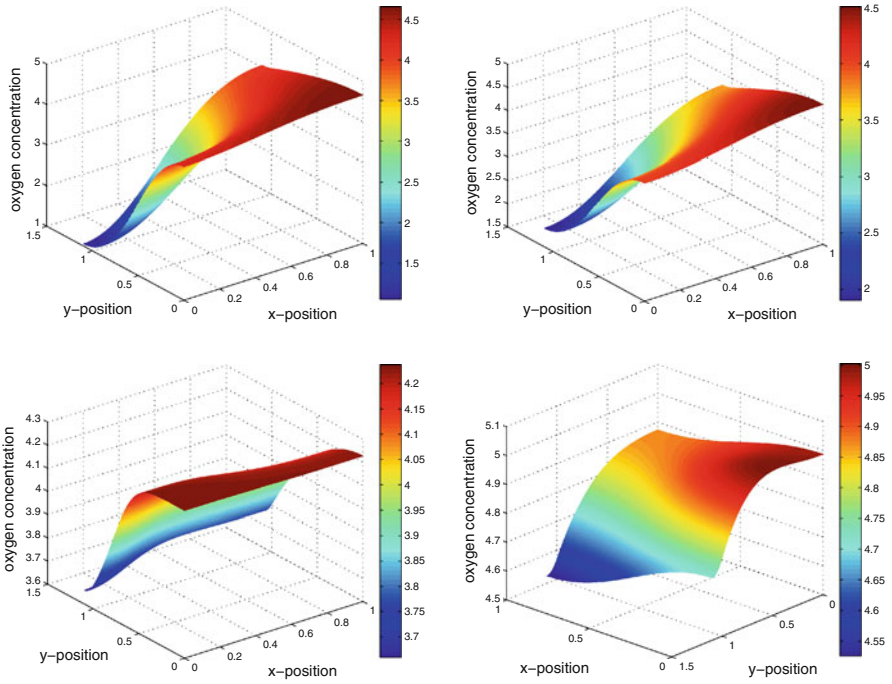

Fig. 6 The oxygen concentration in Ω at days 5, 10, 40 and 100. The figures show the temporal evolution. Here, the position of the basal membrane which connects the dermis to the epidermis coincides with the line $y = 1$. The initial wound occurred at the left. Note that the epidermis is also incorporated

4.2 Angiogenesis simulations

In Fig. 6, we show the oxygen content in the vicinity of the wound at several times. In the undamaged tissue, the oxygen profile resembles the equilibrium profile, whereas in the wounded region, the oxygen content is almost zero and climbs to the equilibrium oxygen tension profile as $t \to \infty$. The low oxygen levels in the wounded region trigger the secretion of the growth factors that stimulate capillary formation. This is perfectly illustrated in Fig. 7, where it can be seen that the VEGF profile exhibits a maximum in the low oxygen region at the wound edge, as a result of the c_{fib}-term in Eq. (13). In Fig. 8, several profiles of the capillary density are shown. At the initial stages, the capillary density is almost zero in the wounded part of the dermis, whereas, at the later stages, the capillary density increases in the wounded part of the dermis due to the relatively high level of VEGF whenever, the (epi-)dermal layer is disrupted. Further, it can be seen that the capillary density is slightly elevated at the rim of the wound. This increase is due to the function ψ, being larger than unity if the fibroblast density is small, and is also observed experimentally. Without the ψ-function, this increase at the wound edge would not be there. The model due to Gaffney et al. features this increase in a more natural way. Further, a more mechano-chemical approach has been described in Murray (2003), although our approach incorporates mechanical effects

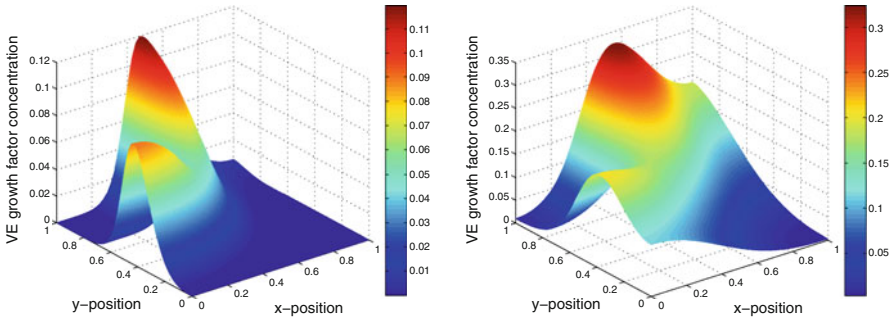

Fig. 7 The VEGF profile in Ω_1 at 5 and 20 days. The figures show the temporal evolution. Here, the position of the basal membrane which connects the dermis to the epidermis coincides with the line $y = 1$. The initial wound occurred at the left

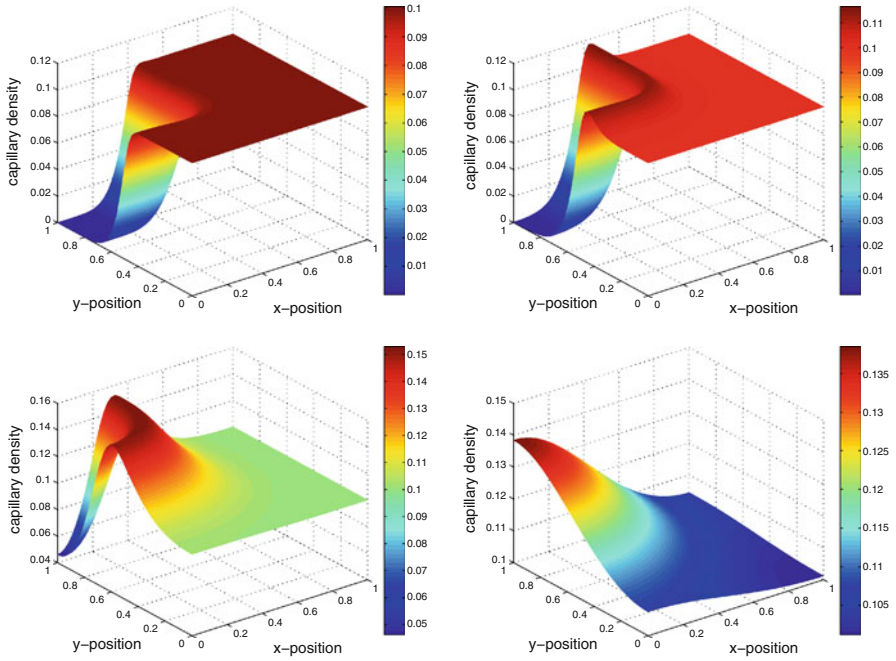

Fig. 8 The capillary profile in Ω_1 at 5, 10, 40 and 100 days. The figures show the temporal evolution. Here, the position of the basal membrane which connects the dermis to the epidermis coincides with the line $y = 1$. The initial wound occurred at the left

as well from the dependence of the diffusion parameters of the capillaries on the local strain tensor.

4.3 Simulations of epidermal closure

In Figs. 9 and 10, the epidermal cell density and epidermal growth factor are plotted at consecutive times. At times just after initiation of reepithelialization, we see that

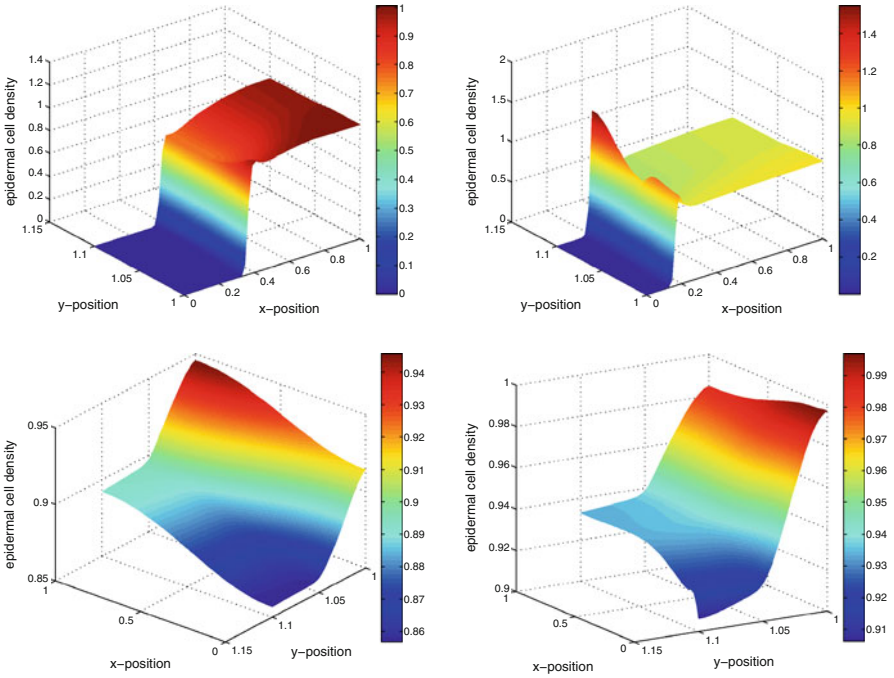

Fig. 9 The epidermal cell density at 5, 10, 40 and 100 days. The figures show the temporal evolution. In the figures, the basal membrane coincides with $y = 1$. Note that **c** and **d** have been rotated for illustrational purposes

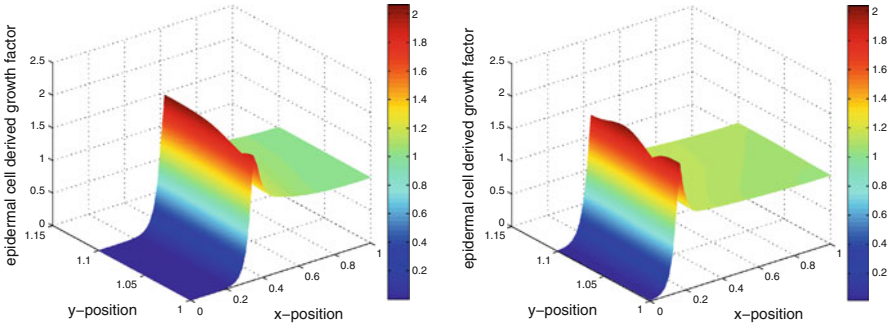

Fig. 10 The epidermal growth factor concentration at 5 and 20 days. The figures show the temporal evolution. The figures show the temporal evolution. In the figures, the basal membrane coincides with $y = 1$

healing of the epidermis progresses away from the undamaged part of the epidermis, so towards the center of the wound, with a peak at the edge during intermediate times. This is also observed experimentally and according to the original simulations due to Sherratt and Murray (1991). At later times, the epidermal cells have moved to the wounded side that is adjacent to the dermis. Then, healing proceeds away in a stratified manner from the basal membrane. This is exactly what happens in clinical situations: healing of the epidermis proceeds from cellular motion from the dermis.

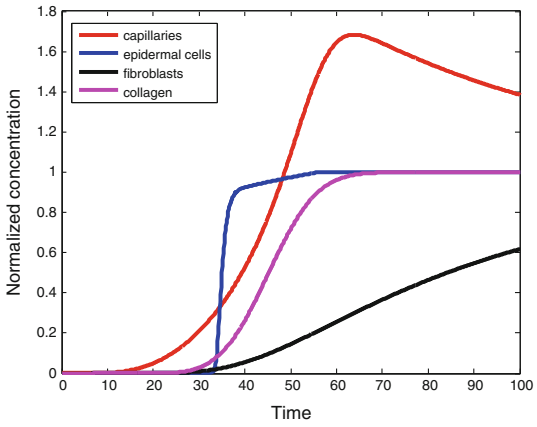

Fig. 11 The concentration in the upper left part of the wound: capillary, ECM, and fibroblast densities at the upper left point of the dermis, epidermal cell density at the upper left point of the epidermis located on the epidermis. Hence, the capillary, ECM and fibroblast densities at position (0, 1) and the epidermal cell density at (0, 1.1)

Sherratt and Murray report a qualitative agreement with experiments conducted on wounds on rabbit's ears, from which the hair follicles were removed, in Murray (2004) and Sherratt and Murray (1991). To get a more quantitative agreement between the model and experiments, regression procedures are desired to get better appropriate values for all model parameters.

4.4 Temporal evolution

In Fig. 11, we show the densities of the fibroblasts, ECM and capillaries in the wound gap. The epidermal cell density on left top position is shown as well. The relatively small values of the fibroblast mobility and ECM diffusivity give rather steep curves for the fibroblast and ECM density. The sequence of the processes is also clearly visible in Fig. 11. It can also be seen that the model allows the partly overlapping of the consecutive processes. We remark that the amount of overlapping is sensitive to the choice of the parameters. Since the healing kinetics of the epidermis largely depend on the oxygen tension, it can be seen that the epidermis heals quite quickly as soon as the oxygen tension is large enough. Further, the small value of the mobility coefficient of epidermal cells results into a sudden increase of the epidermal density. Further, in Fig. 11, it can be seen that the normalized capillary concentration exceeds unity for a while, and that it converges to its equilibrium as $t \to \infty$. The overshoot would never have been obtained if $\phi(c) = 1 \forall c \in \mathbb{R}$. This agrees with the experimentally observed phenomenon of an increased capillary density at the wound edge.

5 Discussion

The current paper describes the mathematical relations and coupling of the processes of wound contraction, dermal regeneration, angiogenesis and wound closure, which all take place during wound healing. The first two mentioned processes take place within the dermis, whereas wound closure evolves in the epidermis. The actual layers were

incorporated in the model by decomposition of the domain of computation. For each of these phenomena, we took some relatively simple models in the current paper, since we aim at a qualitative description of cutaneous wound healing. The present paper is the mathematical modeling counter part of Vermolen and Javierre (2010), in which the lastmentioned paper is extended with a feedback mechanism from angiogenesis (by the local oxygen content) to dermal regeneration.

From the plots in Figs. 9 and 10, it can be seen that re-epithelialization progresses different at the early and later stages of wound closure. At the early stages, see Fig. 9 a, b, wound closure evolves by keratinocyte migration from the undamaged part of the epidermis into the wounded portion of the epidermis, whereas at the later stages, the keratinocytes seem to move in a more layered fashion from the basal membrane, between the epidermis and dermis, directed to the top surface of the epidermis. Note that the plots in Fig. 9c, d have been rotated. This is conforming to what happens in clinical experiments: the first mechanism of healing of the epidermis by climbing of the keratinocytes over each other, and the second mechanism by a construction of adjacent layers parallel to the skin surface (stratification). Our results are confirmed by the experimental studies due to Paddock et al. (2003), Laplante et al. (2001) and Escámez et al. (2004). To give a possible explanation for this phenomenon, we plot the oxygen profile in the epidermis at consecutive times in Fig. 12. It can be seen that the oxygen level decreases in the direction parallel to the basal membrane and hardly changes in the perpendicular direction during the initial stages. However, in the later stages, the change over the direction perpendicular to the basal membrane becomes significant. Comparing with Fig. 10, it is easily observed that the epidermal cell concentration exhibits a similar trend. From our computations, it follows that the epidermal healing evolution is determined by the evolution of the oxygen and nutrients level in the epidermis. Since, the behavior is right from a qualitative point of view, the hypothesis that oxygen and nutrients play an important role in this way, makes sense. At time proceeds, the normalized epidermal cell density converges to unity at all locations in the epidermis. In clinical studies, also an increase of the density of keratinocytes is reported near the moving wound edge. In the current simulations, a very small increase was observed at the early stages. However, as time proceeds, this elevation became smaller. We observed that a change in the oxygen dependence could increase the elevation. Since, we do not model the exact magnitude of this elevation, we did not focus much on this issue. We realize that the present study is only a first attempt to combine several processes in wound healing and to link chemistry, biology and mechanics. To get some feeling of the potential of our formalism, we performed a run with some increased hypothetic values for the cell traction $\tau = 0.5 \times 10^2$ dyne/cell and smaller tethering parameter $s = 10^4$ dyne s/cm^3 to produce Fig. 13, where we show the displacement of mesh nodes near the wound. The figure shows that the upper part of the dermis bulges as it gets swollen as a result of the inflammation. A contraction and retraction behavior was also observed in the one-dimensional simulation of Murray (2004) and in experimental observations that were described there as well. At lower parts in the dermis, the nodes are contracted, which is not clearly visible.

The current model is based on the continuum hypothesis and hence is based on the formulation and solution of PDEs. Despite the random nature of many biological processes, stochastic effects were not incorporated in the present modeling. Every

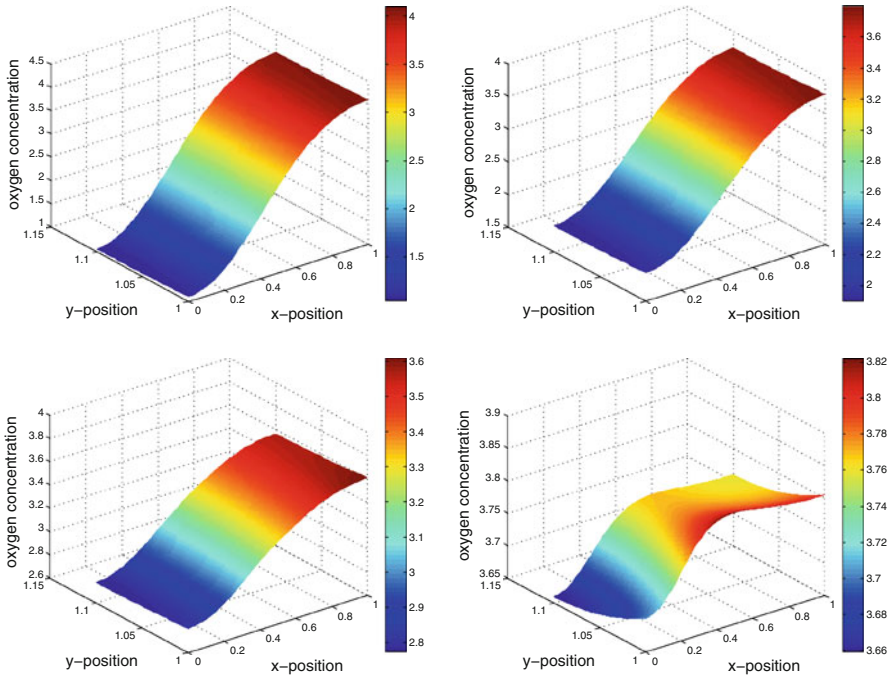

Fig. 12 The oxygen level at 5, 10, 20 and 40 days in the epidermis. The figures show the temporal evolution

Fig. 13 The position of the mesh points where the initial domain was a rectangle of 1×1.2 including both the dermis and epidermis. This shows the swelling of the tissue near the dermal gap at 3.25 days as a result of the forces exerted by the fibroblasts. Note that the cell traction coefficient and tethering coefficients have been unrealistic hypothetic values

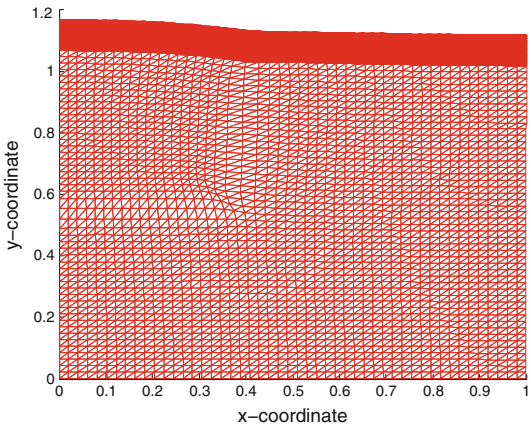

process is assumed to proceed in an ergodic way, and hence only averaged quantities are determined. In future studies, we want to use stochastic finite-elements to solve the model stochastic PDEs. In this way, the uncertainty of many biological parameters can be incorporated and predictions will be made in terms of the evaluation of a probability that a wound heals within a certain timeframe or to evaluate the likelihood that contraction takes place up to certain measure. This latter analysis may be useful for the treatment of burns, where the extent of scar tissue should be minimized for

aesthetic purposes. Despite the interesting picture that the current model gives for the rates, sequence and mutual influence of the various subprocesses taking place during wound healing, still much work remains to be done. For instance, the increase of the capillaries near the wound edge, is modeled in a more natural way by Gaffney et al. (2002), then in the present paper. However, Gaffney et al. (2002) do not incorporate the important initiation of angiogenesis as a result of a depletion of oxygen. A combination of the studies of Gaffney et al. (2002) and Maggelakis (2003), is a topic of future study.

The development of the dermoepidermal junction, which anchors the epidermis on the dermis, has been assumed to be instantaneous. A more thorough understanding of this process is necessary before a mathematical model for this process can be constructed. Some clinicians also argue that the epidermal cells need a good dermoepidermal junction (basal membrane) in order to migrate towards the epidermal wound center. This issue will be studied in collaboration with physicians, since this mechanism could be crucially important. Another issue concerns the communication between the dermis and epidermis. At this moment we assume that only oxygen is responsible for triggering the healing of the epidermis. From discussions with physicians, we know that fibroblasts secrete signaling chemicals that are received by the keratinocytes, thereby triggering healing of the epidermis. This issue will be explored in future and this issue could give a clue in the development of the dermoepidermal junction.

In Murray (2004) and Sherratt and Murray (1991), a qualitative agreement of the model for epidermal regeneration with experiments on rabbit's ears is reported. This model for wound closure is used in the current study. A more complete picture than in the current manuscript for wound contraction or dermal regeneration is presented in Olsen et al. (1995) and Javierre et al. (2009a). In these aforementioned studies, the cell differentiation to myofibroblasts is incorporated, as well as its programmed cell death (apoptosis). The contractile forces that are exerted by the myofibroblast, acting like weak muscle cells, are larger than the forces exerted by the fibroblasts. This differentiation process has been disregarded in the present study, and myofibroblasts are just modeled as fibroblasts here. This was done because we wanted just to take the simplest models that incorporate most of the right biological features in the present study to simulate the coupling of various subprocesses taking place during cutaneous wound healing. We are also aware of the gap in knowledge about parameter values. These simplest models do not predict an increase of the capillaries near the wound edge, as is observed in experimental studies. Furthermore, one should realize that Sherratt's model (Sherratt and Murray 1991) was formulated as a model for epidermal wound closure, where the dermis and basal membrane were assumed to be undamaged. Their aim was to carry out a mathematical analysis in terms of traveling wave solutions. In the future, we tend to co-operate with physicians more in order to shed light on these issues.

In order to bridge between the several partial processes, we plan to carry out a further regression analysis, as well as a further parameter sensitivity analysis based on clinical experiments. A project proposal is being written to collaborate more intensively with physicians in this framework. The current state-of-the-art of our research did not yet incorporate actual and quantitative model validation.

6 Conclusions

The PDEs behind a mathematical model for cutaneous wound healing have been presented. An innovation in this paper is the coupling between the wound contraction, angiogenesis and wound closure, which overlap partly. The healing time of a wound is sensitive to the kinetics of various processes occurring in angiogenesis. However, the kinetics of angiogenesis give a shift of the healing curve, and hence provides an increase of the waiting time before actual healing starts. The model deals with mechanical influences as well, which are of importance when dealing with deeper wounds. Here, the visco-elastic equations have been used. Incorporation of these models, reveals the time response of the sequential processes. The profiles of the capillaries and keratinocytes show the right qualitative behavior in terms of a local increased value at the leading edge. Further, the processes of stratification and climbing over each other by the keratinocytes are reproduced in the simulations of the current paper. Last, but not least, a thorough experimental validation remains crucially important and, therefore, to be incorporated in future studies.

Acknowledgments The financial support by Agentschap, an agency within the Dutch Ministry of Economic Affairs, in the framework of the IOP self-healing materials is gratefully acknowledged. This support enables the fruitful collaboration between the researchers from the Netherlands and Spain. E. Javierre gratefully acknowledges the Spanish Ministry of Science and Innovation through the project DP12009-07514.

References

Adam JA (1999) A simplified model of wound healing (with particular reference to the critical size defect). Math Comput Model 30:23–32

Arnold JS (2001) A simplified model of wound healing III: the critical size defect in three dimensions. Math Comput Model 34:385–392

Balding D, McElwain DLS (1985) A mathematical model of tumour-induced capillary growth. J Theor Biol 114:53–73

Dallon JC (2010) Multiscale modeling of cellular systems in biology. Curr Opin Colloid Interface Sci 15:24–31

Dallon JC, Ehrlich HP (2008) A review of fibroblast populated collagen lattices. Wound Repair Regen 16:472–479

de Vries G, Hillen Th, Lewis M, Müller J, Schönfisch B (2006) A course in mathematical biology: quantitative modeling with mathematical and computational methods. SIAM, Philadelphia

Escámez MJ, García M, Larcher F, Meana A, Nuñoz E, Jorcano JL, Del Rio M (2004) An in vivo model of wound healing in genetically modified skin-humanized mice. J Investig Dermatol 123:1182–1191

Friesel RE, Maciang T (1995) Molecular mechanisms of angiogenesis: fibroblast growth factor signal transduction. FASEB J 9:919–925

Gaffney EA, Pugh K, Maini PK (2002) Investigating a simple model for cutaneous wound healing angiogenesis. J Math Biol 45(4):337–374

Graner F, Glazier J (1992) Simulation of biological cell sorting using a two-dimensional extended Potts model. Phys Rev Lett 69:2013–2016

Hogea CS, Murray BT, Sethian JA (2006) Simulating complex tumor dynamics from avascular to vascular growth using a general level-set method. J Math Biol 53:86–134

Javierre E, Vermolen FJ, Vuik C, van der Zwaag S (2008) Numerical modeling of epidermal wound healing. In: Kunisch K, Of F, Steinbach O (eds) Numerical mathematics and advanced applications. Proceedings of ENUMATH 2007, Berlin. Springer, Berlin, pp 83–90

Javierre E, Moreo P, Doblaré M, García-Aznar MJ (2009a) Computational modelling of wound contraction. In: Proceedings of the Congreso de Métodos Numéricos en Ingeniería 2009, Barcelona. SEMNI

Javierre E, Vermolen FJ, Vuik C, van der Zwaag S (2009b) A mathematical analysis of physiological and morphological aspects of wound closure. J Math Biol 59:605–630

Lamme EN (1999) Artificial skin and tissue regeneration. Thesis, The University of Amsterdam, The Netherlands

Laplante AF, Germain L, Auger FA, Moulin V (2001) Mechanisms of wound reepithelialization: hints from a tissue-engineered reconstructed skin to long-standing questions. FASEB J 15:2377–2382

MacDougall JDB, McCabe M (1967) Diffusion coefficient of oxygen through tissues. Nature 215: 1173–1174

Maggelakis SA (2003) A mathematical model for tissue replacement during epidermal wound healing. Appl Math Model 27(3):189–196

Maggelakis SA (2004) Modeling the role of angiogenesis in epidermal wound healing. Discret Contin Syst 4:267–273

Mantzaris NV, Webb S, Othmer HG (2004) Mathematical modeling of tumor-induced angiogenesis. J Math Biol 49:111–187

Merks MH, Koolwijk P (2009) Modeling morphogenesis in silico and in vitro: towards quantitative, predictive, cell-based modeling. Math Model Nat Phenom 4(4):149–171

Mi Q, Swigon D, Riviere B, Cetin S, Vodorotz Y, Hackam D (2007) One-dimensional elastic continuum model of enterocyte layer migration. Biophys J 93:3745–3752

Murray JD (2003) On the mechanochemical theory of biological pattern formation with application to vasculogenesis. Biol Model 326:239–252

Murray JD (2004) Mathematical biology II: spatial models and biomedical applications. Springer, New York

Olsen L, Sherratt JA, Maini PK (1995) A mechanochemical model for adult dermal wound closure and the permanence of the contracted tissue displacement role. J Theor Biol 177:113–128

Paddock HN, Schultz GS, Mast BA (2003) Methods in reepithalization. In: DiPietro LA, Burns AI (eds) Wound healing methods and protocols. Humana Press Inc., Totowa

Pettet GJ, Byrne HM, McElwain DLS, Norbury J (1996) A model of wound healing angiogenesis in soft tissue. Math Biosci 136:35–63

Plank MJ, Sleeman BD (2003) A reinforced random walk model of tumour angiogenesis and anti-angiogenic strategies. Math Med Biol 20:135–181

Plank MJ, Sleeman BD (2004) Lattice and non-lattice models of tumour angiogenesis. Bull Math Biol 66:1785–1819

Rossiter H, Barresi C, Pammer J, Rendl M, Haigh J, Wagner EF, Tschachler E (2004) Loss of vascular endothelial growth factor A activity in murine epidermal keratinocytes delays wound healing and inhibits tumor formation. Cancer Res 64:3508–3516

Schugart RC, Friedman A, Zhao R, Sen CK (2008) Wound angiogenesis as a function of tissue oxygen tension: a mathematical model. Proc Natl Acad Sci USA 105(7):2628–2633

Sherratt JA, Murray JD (1991) Mathematical analysis of a basic model for epidermal wound healing. J Math Biol 29:389–404

Stadelman WK, Digenis AG, Tobin GR (1997) Physiology and healing dynamics of chronic cutaneous wounds. Am J Surg 176(2):265–385

Stoletov KV, Ratcliffe KE, Terman BI (2002) Fibroblast growth factor receptor substrate 2 participates in vascular endothelial growth factor-induced signaling. FASEB J 16:1283–1285

Swigon D, Arciero J, Mi Q, Hackam D (2010) Continuum elastic model of epithelial sheet migration. Biophys J 93(3) (to appear)

Szpaderska AM, DiPietro LA (2003) In vitro matrigel angiogenesis model. Methods Mol Med 78(1): 311–315

Tranquillo RT, Murray JD (1992) Continuum model of fibroblast-driven wound contraction inflammation-mediation. J Theor Biol 158(2):135–172

Vermolen FJ (2009) A simplified finite-element model for tissue regeneration with angiogenesis. ASCE J Eng Mech 135(5):450–460

Vermolen FJ, Adam JA (2007) A finite-element model for epidermal wound healing. In: Computational Science, ICCS 2007. Springer, Berlin, pp 70–77

Vermolen FJ, Javierre E (2009a) On the construction of analytic solutions for a diffusion–reaction equation with a discontinuous switch mechanism. J Comput Appl Math 231:983–1003

Vermolen FJ, Javierre E (2009b) A suite of continuum models for different aspects in wound healing. In: Gefen A (ed) Bioengineering research of chronic wounds, studies in mechanobiology, tissue engineering and biomaterials. Springer, Berlin

Vermolen FJ, Javierre E (2010) Computer simulations from a finite-element model for wound contraction and closure. J Tissue Viability 19:43–53

Wearing HJ, Sherratt JD (2000) Keratinocyte growth factor signalling: a mathematical model of dermal–epidermal interaction in epidermal wound healing. Math Biosci 165:41–62

Xue C, Friedman A, Sen CK (2009) A mathematical model of ischemic cutaneous wounds. Proc Natl Acad Sci USA 106(39):16783–16787